ARTICLES

Structure Formation of Hydrophobically End-Capped Poly(ethylene oxide) in the Solid State

Young-Wook Choi,[†,§] Jaehyun Park,[†,||] Youngmi Park,[†] Kyungbae Kim,[†] Youngil Lee,[‡] and Daewon Sohn*[,†]

Department of Chemistry, Hanyang University, Seoul 133-791, Korea, and Department of Chemistry, University of Ulsan, Ulsan 680-749, Korea

Received: June 11, 2007; In Final Form: August 21, 2007

The conformational transition of hydrophobically end-capped poly(ethylene oxide), HP-PEO-HP [hydrophobic-poly(ethylene oxide)-hydrophobic], was studied using X-ray diffraction (XRD), differential scanning calorimetry (DSC), and Fourier transform infrared spectroscopy (FTIR) methods. Conformational transitions of HP-PEO-HP from a planar zigzag to a 7/2 helical conformation were observed as the molecular weight of the PEO main chain increased. HP-PEO-HP 1(18), with a PEO molecular weight of 1000 and 18 hydrocarbons on each end, has mainly an α-helical structure in poor solvents, whereas α and β conformations coexist in good solvents. This means that the α-helical structure caused by the hydrogen bonds between the urethane linkages was broken by the high chain mobility caused by the melted adjacent chains of PEO, and instead, the β-sheet was formed by the interaction of multiple hydrogen bonds. Another indication of hydrogen bonds breaking at increasing temperature is the transition of the N−H stretching peak in the FTIR data. HP-PEO-HP 2(18) and 4(18), which have 18 hydrocarbons on each end and PEO molecular weights of 2000 and 4000, respectively, and consist mostly of PEO, showed spherulites. This result also suggests that the PEO molecule has a 7/2 zigzag helical conformation. In contrast, HP-PEO-HP 1(18), which is composed of less PEO than HP-PEO-HP 2(18) and 4(18), did not show a spherulite structure.

Introduction

The creation of supramolecular structures with well-defined shapes and functions is one of the many fascinating subjects in the areas of material science, nanochemistry, and biomedical chemistry.[1] Self-assembly of molecules through noncovalent forces including hydrophobic and hydrophilic effects, electrostatic interactions, hydrogen bonding, and microphase segregation has great potential for creating such supramolecular structures.[2−6] To prepare a well-defined supramolecular structure, unique diblock and triblock copolymer structures have been investigated by many research groups.[7] An interesting block polymer is PE/PEO [poly(ethylene)/poly(ethylene oxide)] because the PE and PEO blocks normally adopt different crystal structures.[8] PE typically crystallizes in an orthorhombic unit cell with a planar zigzag conformation, whereas PEO crystallizes as a 7/2 helix, although the metastable PEO phase still contains a planar zigzag conformation.[9−11] Recently, the triblock oligomer $[H(CH_2)_m(CH_2CH_2O)_n(CH_2)_mH]$ was studied by the Baker group.[12] They found that, for $n < 7$ ($m = 12-20$), the EO (ethylene oxide) segment is in a planar zigzag conformation, whereas for $n > 7$, the EO segment crystallizes in the 7/2 helical conformation.[8,12]

The representative water-soluble ABA-type polymer surfactant, hydrophobically end-capped poly(ethylene oxide) (HP-PEO-HP), consists of one hydrophilic poly(ethylene oxide) (PEO) middle chain and two hydrophobic end groups attached by a urethane bond.[13] It is known that the water-insoluble alkyl end chains of HP-PEO-HP associate to form micelle-like clusters at the critical micelle concentration (CMC).[14,15] That is, HP-PEO-HP unimers form flowerlike micelles with hydrophobic cores surrounded by hydrophilic poly(ethylene oxide) shells. These associations, however, can be altered by varying the molecular weight, the polydispersity index of the polymer, the presence of a urethane group between the end chain and the main chain, the length of the hydrophobic end chain, and the length of hydrophilic main chain.[16−18] A number of research groups have extensively examined the properties of aqueous HP-PEO-HP solutions,[13−18] but few studies on the solid state of HP-PEO-HP have been reported. Conformational studies of HP-PEO-HP in the solid state have yielded the discovery of a unique feature: hydrogen bonding in urethane can play an important role in the formation of a supramolecular structure. Recently, we showed that the increased crystallinity due to the intermolecular interactions of the PEO main chains increases the affinity of the end hydrocarbons and results in a phase transition from the trans to gauche form.[19]

In this article, we demonstrate effects of the main chain and the solvent on the HP-PEO-HP crystallization process using

* Corresponding author. E-mail: dsohn@hanyang.ac.kr. Tel.: +82-2-2220-0933. Fax: +82-2-2299-0762.
† Department of Chemsitry, Hanyang University, Seoul, 133-791, Korea.
‡ Department of Chemistry, University of Ulsan, Ulsan, 680-749, Korea.
§ Current address: R & D Center, LG Micron, 1271, Sa 1-dong, Sangrok-gu, Ansan 426-791, Korea.
|| Current address: R & D Center, SK Energy Co., 140-1, Wonchon-dong, Yuseong-gu, Daejeon 305-712, Korea.

10.1021/jp074496j CCC: $37.00
Published on Web 10/24/2007

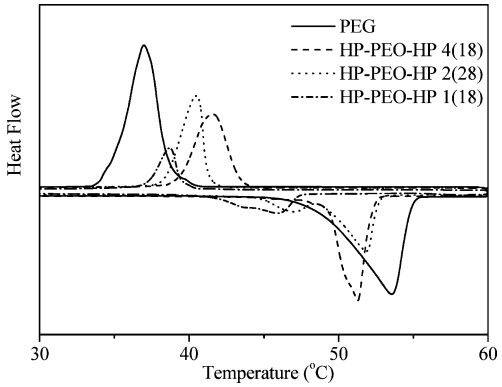

Figure 1. DSC heating traces (first heating cycle, 10 °C/min) for PEO (solid line), HP-PEO-HP 4(18) (dashed line), HP-PEO-HP 2(18) (dotted line), and HP-PEO-HP 1(18) (dash-dotted line).

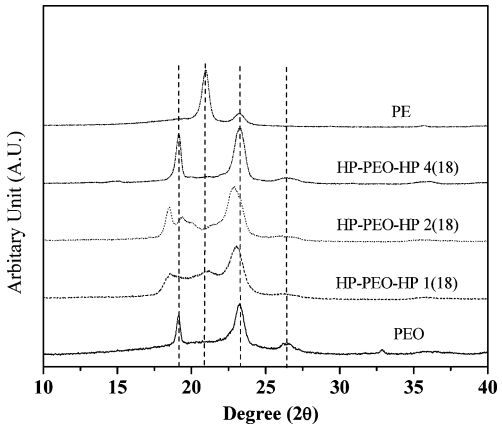

Figure 2. Wide-angle X-ray diffraction patterns of PEO, PE, and the HP-PEO-HP series.

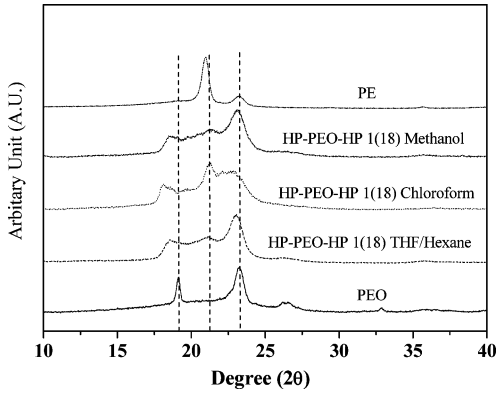

Figure 3. Wide-angle X-ray diffraction patterns of HP-PEO-HP 1(18) prepared in different solvents.

several spectroscopic methods. HP-PEO-HP molecules having a PEO segment with various molecular weights (1000, 2000, 4000) and two end groups of urethane bonds with alkyl lengths of $n = 18$ [HP-PEO-HP 1(18), HP-PEO-HP 2(18), HP-PEO-HP 4(18), respectively] were used.

Experimental Section

Materials. Poly(ethylene oxide) (PEO, $M_w = 1000$, 2000, and 4000 g/mol, PDI = 1.1) was purchased from Fluka. Octyl isocyanate was purchased from Aldrich. Details of HP-PEO-HP synthesis and characterization can be found in a previous work.[16] HP-PEO-HP 1(18), HP-PEO-HP 2(18), and HP-PEO-HP 4(18) denote the materials synthesized with PEO molecular weights of 1000, 2000, and 4000 Da, respectively, all with octadecyl hydrocarbon groups on both ends.

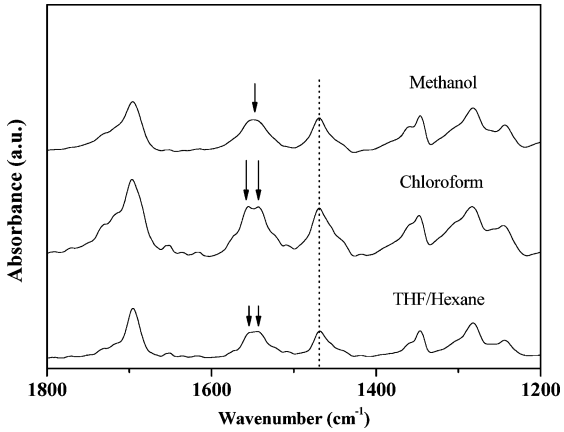

Figure 4. FTIR spectra of HP-PEO-HP 1(18) prepared in the solvents THF/hexane, chloroform, and methanol.

Differential Scanning Calorimetry. A Mettler Toledo Star DSC instrument, capable of programmed temperature cycling over the range from −110 to 300 °C, was used. Samples were first heated to the melting point at a rate of 10 °C/min and subsequently cooled to −30 °C at the same rate. The transition temperatures and enthalpies were obtained by a second heating at the same rate.

Fourier Transform Infrared Spectroscopy. Absorbance FTIR experiments were carried out with a Bio-Rad FTS-6000 temperature-controlled accessory. The temperature was controlled from 25 to 125 °C, and the spectrum was acquired with 2-nm resolution.

X-ray Diffraction. Wide-angle X-ray diffraction (WXRD) measurements were performed with a Shimadzu XRD-6000 instrument. The 1.54-Å Cu Kα radiation from a Siemens generator operating at 35 kV and 30 mA was used. Measurements were made in the 2θ range from 0.1° to 40° in steps of 0.1°.

Molecular Dynamics Simulations. Atomistic molecular dynamics simulations using the MMFF force field were employed to investigate the structural effects of HP-PEO-HP. For convenience, each model was abbreviated. The HP-PEO-HP molecules all had the trans 7/2 helical conformation. The generated structure was minimized to find a stable conformation.

Results and Discussion

The DSC results for HP-PEO-HP 1(18), HP-PEO-HP 2(18), and HP-PEO-HP 4(18) are shown in Figure 1.

There were considerable differences between the melting curve and the recrystallization curve. Typical PEO ($M_w = 2000$ g/mol) showed only a single broad melting peak near 55 °C, but all HP-PEO-HPs exhibited a shoulder peak in the melting curve. HP-PEO-HP 1(18) had a broad melting curve between 40 and 50 °C and showed a shoulder peak near 42 °C. HP-PEO-HP 2(18) had two melting curves near 45 and 55 °C, whereas HP-PEO-HP 4(18) showed a relatively sharp melting curve between 47 and 53 °C along with a shoulder peak near 50 °C. Recrystallization curves showed some regular features according to changes in the main chain, PEO composition, and molecular weight. The recrystallization temperature decreased as the molecular weight of the main chain decreased. Because the melting temperature of PE is higher than that of PEO, the DSC data suggest that the conformation of the HP-PEO-HP materials is the same as the mixed PE and PEO conformation.

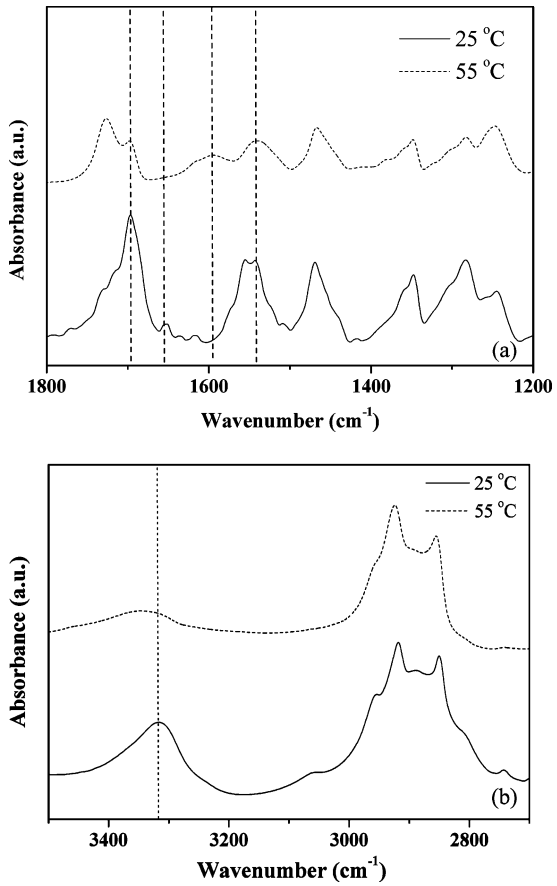

Figure 5. Variable-temperature FTIR spectra of HP-PEO-HP 1(18) near (a) the amide I and II bands and (b) the N−H stretching band at 25 and 55 °C.

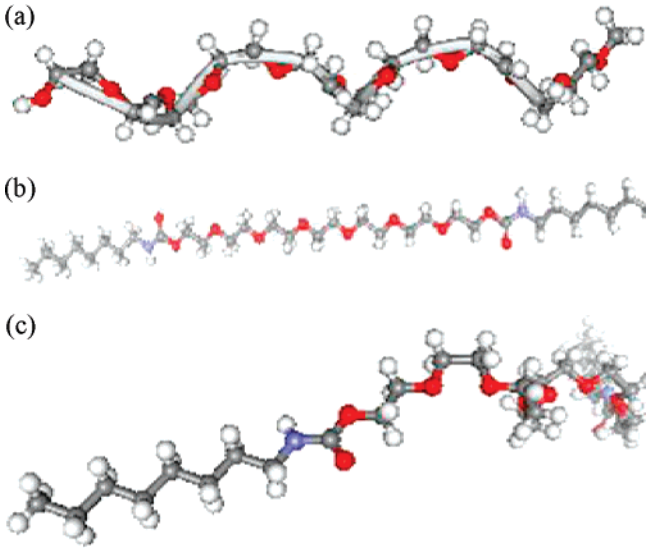

Figure 6. Computational model of (a) the 7/2 helical conformation of PEO, (b) the all-trans conformation of HP-PEO-HP, and (c) the tilted 7/2 helical conformation of HP-PEO-HP.

That is, a mixture of the zigzag and the 7/2 helical structures is present in HP-PEO-HP. This is called the 7/2 helix of the PEO crystal. To study in detail the effects of the main-chain length on the structural transition, XRD experiments were performed. WAXD patterns of all HP-PEO-HP samples are displayed in Figure 2. Figure 2 clearly shows the effect of the main-chain length. HP-PEO-HP 2(18) and 4(18) have peak positions similar

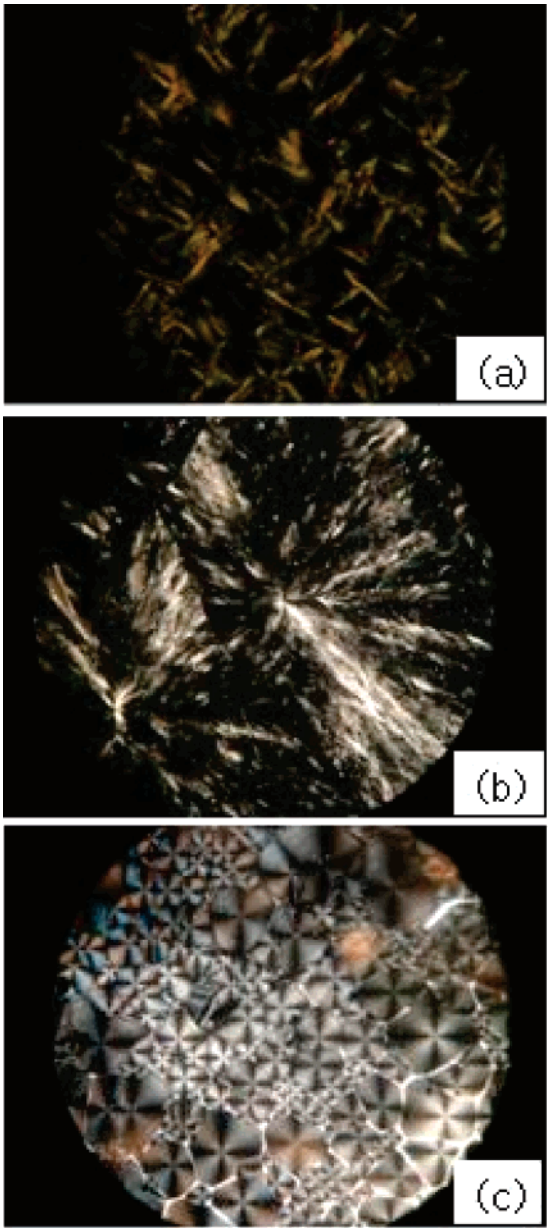

Figure 7. Polarized optical microscopy images of (a) HP-PEO-HP 1(18), (b) HP-PEO-HP 2(18), and (c) HP-PEO-HP 4(18).

to those of PEO, whereas HP-PEO-HP 1(18) has a mixed peak position between those of PE and PEO.

The WAXD patterns at 19°, 23°, and 26° are characteristic of PEO crystals in which the PEO chains form a 2/7 helix structure,[20] and the WAXD patterns at 21° and 23° are characteristic of PE crystals in which the PE chains form a zigzag conformation. HP-PEO-HP 1(18) has broad XRD peaks between 20° and 25°, and shows a shoulder peak near 21°. HP-PEO-HP 2(18) has broad XRD peaks between 20° and 25° and shows only a small shoulder peak near 21°. HP-PEO-HP 4(18) has sharp XRD peaks, similar to the pure PEO peaks. XRD suggests that, although HP-PEO-HP has a conformation much more complicated than a simple mixture of PE and PEO conformations because of hydrogen-bonding interactions and conformational restrictions of urethane linkages, basically the conformation of the HP-PEO-HP materials is a mixed PE and PEO conformation, with both the zigzag and 7/2 helical structures coexisting in HP-PEO-HP. As the molecular weight of the PEO main chain increased, the conformation of HP-PEO-

HP transformed from a 7/2 helical conformation to a planar zigzag conformation.

To explain a helical or trans conformation for the PEO core under different crystallization conditions, Chen et al. adopted a stepwise process for the crystallization of ABA oligomers.[8] These molecules adopt their normal planar zigzag conformations. That is, in hydrophobic solvents, the alkyl portions of the oligomers should be more soluble than the PEO core, and the less soluble PEO core should crystallize first while selecting its most stable conformation, the 7/2 helix. When the alkyl fragments crystallize, they tilt with respect to the PEO core axis to accommodate the helical structure of the PEO core and to increase the packing density.

Figure 3 shows the XRD data of HP-PEO-HP crystalline structures prepared in different solvents. HP-PEO-HP 1(18) prepared in THF/hexane or methanol has a broad XRD peak between 20° and 25° and a shoulder peak near 21°, similarly to pure PEO. Both solvents are poor solvents for HP-PEO-HP 1(18), and thus, crystallization is likely a fast process. On the other hand, chloroform is a good solvent for HP-PEO-HP 1(18) and is likely to slow the crystallization process. HP-PEO-HP 1(18) showed different characteristics than did HP-PEO-HP 2(18) and HP-PEO-HP 4(18). The competition between the PEO main chain and the alkyl end chains is predominant for HP-PEO-HP 1(18). To investigate the solvent-dependent secondary structures of HP-PEO-HP 1(18), IR spectroscopy experiments were carried out with samples prepared in different solvents. Figure 4 shows FTIR spectra of HP-PEO-HP 1(18) prepared in the solvents THF/hexane, chloroform, and methanol.

Figure 4 shows similar peaks in the different solvents. The only distinguishable peak comes from the amide II band near 1550 cm^{-1}. HP-PEO-HP 1(18) does not clearly show the peaks of amide I near 1650 cm^{-1}, but amide II near 1550 cm^{-1} is visible as seen in Figure 4. HP-PEO-HP 1(18) in an unfavorable solvent shows an amide II peak near 1550 cm^{-1} that is characteristic of an α-helical structure,[21,22] whereas the amide II band of HP-PEO-HP 1(18) in a favorable solvent, chloroform, is separated into peaks at 1560 and 1540 cm^{-1}, as indicated by two long arrows. The β-sheet conformation has an amide II peak near 1540 cm^{-1}, which was assigned to an increased H-bond strength.[23] In addition, the characteristic CH_2 bending peaks of the PEO helical conformation are near 1470 and 1280 cm^{-1}, and the CH_2 torsion peak of the PE/PEO mixed conformation is near 1350 cm^{-1}.[12] The C═O stretching peak near 1680 cm^{-1} was not affected by variations in the PEO content of the compounds. XRD and FTIR studies of HP-PEO-HP 1(18) in different solvents provided clear evidence for the assumption that HP-PEO-HP 1(18) in a poor solvent has mainly an α-helical structure whereas the α and β conformations coexist in a good solvent.

To investigate the conformational transition of HP-PEO-HP 1(18), variable-temperature IR spectroscopy experiments were performed. Figure 5 shows the variable-temperature FTIR spectra of HP-PEO-HP 1(18) near (a) the amide I and II bands and (b) the N−H stretching band at 25 and 55 °C.

As mentioned in regard to Figure 4, HP-PEO-HP 1(18) has a mixed conformation when slowly dried in a good solvent. Figure 5a shows distinguishable peak shifts about the amide I and II bands. As the temperature is increased, the small shoulder peaks of amide I near 1650 cm^{-1} and amide II near 1550 cm^{-1} disappear, whereas the amide II band near 1540 cm^{-1} increases. This means that the α-helical structure caused by the intramolecular interactions of hydrogen bonds was broken by the high chain mobility resulting from the melted adjacent chains of PEO and, instead, a β-sheet was formed by the interactions of multiple hydrogen bonds.[24] Another good indication for the breaking of hydrogen bonds with increased temperature is the transition of the N−H stretching peak. The broad band near 3320 cm^{-1} that results from intermolecular hydrogen bonding shifts toward the high-wavenumber region and decreases in intensity.[25]

Figure 6 shows the computational model of (a) the 7/2 helical conformation of PEO, (b) an all-trans conformation of HP-PEO-HP, and (c) a tilted 7/2 helical conformation of HP-PEO-HP. In the case of the 7/2 helical conformation of PEO, the torsion angle of O−C−C−O is about 70°, whereas the torsion angle of O−C−C−O of trans PEO is 180°. As shown Figure 6c, HP-PEO-HP shows a tilted trans or 7/2 helical conformation because of the coexistence of the trans conformation of the alkyl chain and the helical conformation of PEO. The relatively short main chain in HP-PEO-HP 1(18) could result in a less rigid structure than the trans zigzag conformation of long main chains as in HP-PEO-HP 2(18) and HP-PEO-HP 4(18). Therefore, as shown in Figure 7c, HP-PEO-HP shows a tilted trans or 7/2 helical conformation because of the coexistence of the trans conformation of the alkyl chain and the helical conformation of PEO. In detail, the first and second PEO units have trans conformations, but the third PEO unit shows a helical conformation, so the overall structure of low-molecular-weight HP-PEO-HP could be bent.

Until now, we have discussed the conformation transition of HP-PEO-HP in terms of its dependence on the main chain, solvent, and temperature. As the content of PEO increased, HP-PEO-HP followed original PEO behavior, but HP-PEO-HP 1(18) showed a structural transition with respect to solvent solubility and temperature, because of the strong interference between the trans conformation of the alkyl chain and the 7/2 helical conformation of the PEO main chain.

Spherulite is characteristic of high-molecular-weight PEO;[20] therefore, HP-PEO-HP 2(18) and 4(18), which contain long PEO chains, showed spherulites. This result also suggests that the PEO molecule has a 7/2 zigzag helical conformation in HP-PEO-HP 2(18) and 4(18), whereas HP-PEO-HP 1(18), which included a smaller amount of PEO, showed a smectic phase because of the stacking of the trans conformation. Figure 7 shows the polarized optical microscopy images of (a) HP-PEO-HP 1(18), (b) HP-PEO-HP 2(18), and (c) HP-PEO-HP 4(18).

Acknowledgment. This work was supported by the research fund from the National R & D Project for Nano Science and Technology in Korea (KISTEP). D.S. is grateful to the ABRL program of KOSEF (Grant R-14-2002-004-01002-0). K.K. acknowledges the BK21 program in Korea.

References and Notes

(1) Lee, M.; Cho, B.-K.; Zin, W.-C. *Chem. Rev.* **2001**, *101*, 3869.
(2) Whitesides, G. M.; Mathias, J. P.; Seto, C. P. *Science* **1991**, *254*, 1312.
(3) Lehn, J. M. *Supramolecular Chemistry*; VCH: Weiheim, Germany, 1995.
(4) Muthukumar, M.; Ober, C. K.; Thamas, E. L. *Science* **1997**, *277*, 1225.
(5) Foster, S.; Antonietti, M. *Adv. Mater.* **1998**, *10*, 195.
(6) Israelachvili, J. *Intermolecular and Surface Forces*; Academic Press: London, 1992.
(7) Bates, F. S.; Fredrickson, G. H. *Annu. Rev. Phys. Chem.* **1990**, *41*, 525.
(8) Chen, Y.; Baker, G. L. *J. Am. Chem. Soc.* **1999**, *121*, 6962.
(9) Takahashi, Y.; Tadokoro, H. *Macromolecules* **1973**, *6*, 881.
(10) Takahashi, Y.; Sumita, I.; Tadokoro, H. *J. Polym. Sci. B: Polym. Phys.* **1973**, *11*, 2113.
(11) Tashiro, K.; Tadokoro, H. *Rep. Prog. Polym. Phys. Jpn.* **1978**, *21*, 417.

(12) Ding, Y.; Rabolt, J. F.; Chen, Y.; Olson, K. L.; Baker, G. L. *Macromolecules* **2002**, *35*, 3914.

(13) Rao, B.; Umera, Y.; Dyke, L.; Mcdonald, P. M. *Macromolecules* **1995**, *28*, 531.

(14) Yekta, A.; Xu, B.; Duhamel, J.; Winnik, M. A. *Macromolecules* **1995**, *28*, 956.

(15) Maechling-Strasser, C.; Clouet, F.; Francois, J. *Polymer* **1992**, *33*, 627.

(16) Paeng, K. W.; Kim, B. S.; Kim, E. R.; Sohn, D. *Bull. Korean Chem. Soc.* **2000**, *21*, 623.

(17) Kim, M.; Choi, Y.-W.; Sim, J.-H.; Choo, J.; Sohn, D. *J. Phys. Chem. B* **2004**, *108*, 8269.

(18) Chassenieux, C.; Nicolai, T.; Durand, D. *Macromolecules* **1997**, *30*, 4952.

(19) Lee, Y.; Choi, J.; Choi, Y.-W.; Sohn, D. *J. Phys. Chem. B* **2003**, *107*, 12373.

(20) Tanaka, S.; Ogura, A.; Kaneko, T.; Murata, Y.; Akashi, M. *Macromolecules* **2004**, *37*, 1370.

(21) Miyazawa, T.; Blout, E. R. *J. Am. Chem. Soc.* **1961**, *83*, 712.

(22) Kubelka, J.; Keiderling, T. A. *J. Am. Chem. Soc.* **2001**, *123*, 6142.

(23) Floudas, G.; Papadopoulos, P.; Klok, H.-A.; Vendermeulen, G. W. M.; Rodriguez-Hernandez, J. *Macromolecules* **2003**, *36*, 3673.

(24) Tanaka, S.; Ogura, A.; Kaneko, T.; Murata, Y.; Akashi, M. *Macromolecules* **2004**, *37*, 1370.

(25) Gellman, S. H.; Dado, G. P.; Liang, G.-B.; Adams, B. R. *J. Am. Chem. Soc.* **1991**, *113*, 1164.